Inhomogeneous lens antenna design with fan-beam radiation pattern

Mohammad Mahdi Taskhiri* and Mohammad Khalaj-Amirhosseini

School of Electrical Engineering, Iran University of Science and Technology, Tehran 1684613114, Iran

**Corresponding author: mm.taskhiri@ee.iust.ac.ir*

Received May 27, 2016; accepted October 21, 2016; posted online November 21, 2016

This Letter presents an original technique to design and synthesize an inhomogeneous asymmetrical lens resulting in a special fan-beam radiation pattern in a wide frequency bandwidth. The vertical and horizontal planes of the fan-beam radiation pattern can be determined separately. Wide angle search and detection are achievable by using this type of lens antenna because of its suitable radiation pattern. The proposed relative index profile is validated by the means of commercial CST software and an FDTD scheme.

OCIS codes: 160.3918, 080.0080, 080.3630, 080.5692, 110.2760, 230.7370.

doi: 10.3788/COL201614.121601.

In recent years, lens antenna systems have been widely used in many applications, such as point-to-point and point-to-multi-point links, automotive radar, Doppler-weather radar, aircraft landing systems, radio astronomy, satellite communications, radio frequency identification, imaging systems at millimeter waves, access control and security, product tracking, logistics, and public transportation. In the literature, researchers have reported many lens antenna based on their working principles. However, the potential of lens antenna seems does not seem to have been fully reached yet.

Lens utilization is a method to improve the gain and side-lobe level (SLL) of feeding antennas[1–4] and can be used in scattering applications[5].

In general, lens antennas can be separated into two categories: homogeneous[6] and inhomogeneous index profiles. There are some methods to realize inhomogeneous lenses, such as material drilling[7–11], PCB techniques[12,13], wire grids[14,15], multilayers[16–18], and other methods[19–22].

The Luneburg lens[23] is an inhomogeneous symmetrical spherical lens where the relative index profile (n) varies with the square of the radius, $n = \sqrt{2-(r/R)^2}$, where r is the radius from the center point and R is the outer radius of the lens. This type of lens is very useful in antenna and scattering applications[7,13,24].

The Luneburg lens design is extracted from the transformation optics theory. Transformation optics is a method to design lens antennas that is realized by controlling the electromagnetic field at the desired coordinates to obtain complex materials[25–28].

The lenses in most of the mentioned Letters have a symmetrical shape and index profile. So the radiation pattern of a three-dimensional (3D) model lens is the same as a pencil beam. Two-dimensional (2D) model realization is more convenient than 3D model realization, so the radiation pattern of a planar form fabrication lens is like a fan-beam pattern. It produces a beam that is wide in the narrow plane and narrow in the wide plane of an asymmetrical lens. In this type of planar model, the control of the beam width is possible in one plane, but there is no control over the other planes of the radiation pattern beam width.

Wide angle searches are required in some modern radar and satellite systems operating at millimeter-wave and microwave-frequency bands, such as weather radar, tracking systems, and remote sensing applications. Parabolic reflectors and array antennas can be designed to radiate asymmetrical patterns in vertical and horizontal planes because of their special shape and feeding structures.

In this Letter, a broad-band inhomogeneous asymmetrical lens is presented based on geometric optics and the Eikonal equation[29], resulting in a special fan-beam radiation pattern. The vertical and horizontal planes of this fan-beam radiation pattern can be controlled separately. This is the main improvement of this method compared to others based on transformation optics. It is suitable to have a lens antenna that works in a broad-band frequency application. This feature is another aspect that is considered in this method. We design a 3D asymmetrical lens that has a fan-beam radiation pattern in which the half-power beam width of the pattern in the narrow plane is twice that in the wide plane.

The size of the lens antenna is approximately inversely proportional to the free-space wavelength. So, the size of the antenna is reduced at mm wavelengths. The center frequency of operation is considered equal to 10 GHz for a 3D asymmetrical lens.

First, the refractive index of the inhomogeneous asymmetrical lens is proposed, based on geometric optics and the Eikonal equation. Then, the proposed refractive index is validated in some cutting planes by using the FDTD scheme. The refractive index profile is approximated in CST commercial software, and the performance of the radiation pattern for this type of lens is discussed.

A fan-beam radiation pattern can result from a lens antenna having an asymmetrical aperture. A typical structure of this type of lens is shown in Fig. 1, which has an elliptical aperture with diameters $2a$ and $2b$. It is assumed

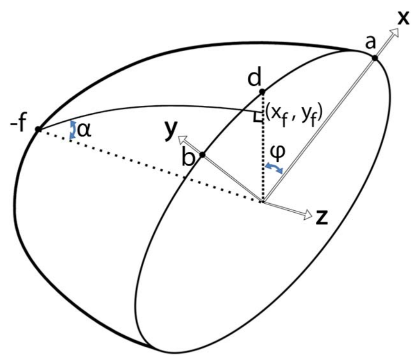

Fig. 1. Typical structure of an inhomogeneous and asymmetric lens.

that the refractive index is inhomogeneous and has a continuous and gradual change. So, to analyze the lens, we consider it as many planes, all of them crossing the z-axis. The length of theoutput side of each plane is $2d$, which is between $2a$ for the XZ plane and $2b$ for the YZ plane. The lens is excited by a point source located at point $(0, 0, -f)$. The point source emits many rays of rising angle α with respect to the z-axis, as shown in Fig. 2.

Ray optics formulas in inhomogeneous, isotropic, lossless media were defined in the form of the Eikonal equation[29,30] as

$$n^2(\rho, z) = \dot{\rho}^2 + \dot{z}^2 = \left(\frac{\partial \rho}{\partial t}\right)^2 + \left(\frac{\partial z}{\partial t}\right)^2. \tag{1}$$

Here, we choose a general nonuniform function of ρ and z related to t with at least 9 unknown constants for the ray trajectory in the ρz plane (see equation below). The unknown constants are determined to satisfy all conditions, which will be explained later. Then we have

$$\begin{cases} z(t) = M_1 \sin\left(p\frac{t}{t_f}\right) + M_2 \cos\left(p\frac{t}{t_f}\right) + M_3 \\ \rho(t) = N_1 \sin\left(q\frac{t}{t_f}\right) + N_2 \cos\left(q\frac{t}{t_f}\right) + N_3 \end{cases}, \tag{2}$$

where $M_1, M_2, M_3, N_1, N_2, N_3, p, q,$ and t_f are unknown parameters. The variable t varies from 0 to t_f for the source and output points, respectively. The parameter t_f is the final value of the variable t that the ray reaches the endpoint for a starting angle equal to α.

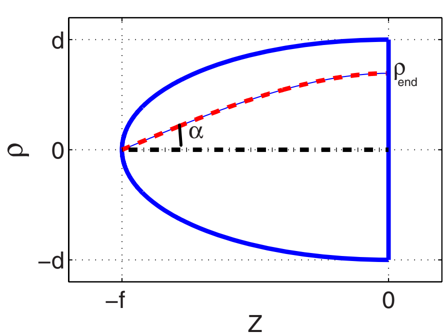

Fig. 2. Sample plane cross-section view of asymmetrical lens, whose thickness and aperture diameter are f and $2d$. Each beam ray leaves from a point source at an angle α with respect to the z-axis and propagates through the lens.

The lens antenna must convert a spherical or cylindrical wavefront produced, respectively, by a point or line source feed, into an outgoing planar or linear wavefront. All the output beam rays in each plane of the asymmetrical lens must be collimated to the output plane normal vector (z-axis) and have same phase as each other. Also, to access a more efficient radiation pattern with the maximum gain and directivity, the distance between the ray's endpoints must be uniformly distributed on the output boundary for a point source antenna.

We want to design a lens antenna that works in a broadband frequency bandwidth. So, the refractive index of the lens must be equal to one in proximity to the point source and the surrounding space (on the $z = 0$ plane).

To determine the unknown constants in Eq. (2), the following conditions are used step by step for all rays lying on each plane of asymmetric lens, separately. Each ray must have three groups of conditions as follows:

1. At the starting or exciting point, $t = 0$, the following four conditions are there, assuming a matched exciting point, i.e., $n = 1$,

$$\begin{cases} z = -f; \rho = 0 \\ \frac{\partial \rho}{\partial z} = \frac{\dot{\rho}}{\dot{z}} = \tan(\alpha) \\ \dot{\rho}^2 + \dot{z}^2 = 1 \end{cases}. \tag{3}$$

2. At the end point or on the aperture of diameter $2d$, $t = t_f(\alpha)$, the following four conditions are there, assuming parallel rays, matched apertures, i.e., $n = 1$, and a uniform power distribution on the aperture,

$$\begin{cases} z = 0; \rho = \rho_{\mathrm{end}}(\alpha) = \frac{2\alpha}{\pi} d \\ \dot{\rho} = 0; \dot{z} = 1 \end{cases}, \tag{4}$$

where $d = \frac{ab}{\sqrt{a^2 \sin^2 \varphi + b^2 \cos^2 \varphi}}$.

3. The electric phases of all rays on the output plane must be equal to each other, so

$$l_e(\alpha) = \frac{c\Delta\phi}{\omega} = \int n(\rho, z)\mathrm{d}s = \int n\sqrt{(d\rho)^2 + (\mathrm{d}z)^2} = \int n\sqrt{\dot{\rho}^2 + \dot{z}^2}\mathrm{d}t = \int_0^{t_f(\alpha)} n^2(\alpha, t)\mathrm{d}t = \text{cte.}, \tag{5}$$

where $\Delta\phi$ is the electric phase corresponding to an axial ray. It is better to choose as small a value as possible.

The conditions in Eqs. (3) and (4), give, respectively, the following equations, for the unknown coefficients:

$$\begin{cases} M_3 = -f - M_2, N_3 = -N_2 \\ M_1 = \frac{t_f \cos(\alpha)}{p}, N_1 = \frac{t_f \sin(\alpha)}{q} \end{cases}, \tag{6}$$

$$\begin{cases} M_2=\dfrac{pf-t_f\cos(\alpha)\sin(p)}{p(\cos(p)-1)}, N_2=\dfrac{q(\frac{2\alpha}{\pi}d)-t_f\sin(\alpha)\sin(q)}{q(\cos(q)-1)} \\ \tan(p/2)(t_f(\cos(\alpha)+1))=pf, \tan(q/2)(t_f\sin(\alpha))=q\left(\frac{2\alpha}{\pi}d\right). \end{cases} \tag{7}$$

According to Eq. (6) and (7), only one parameter (t_f) remains unknown and determinant. This parameter is chosen so as to have the minimum optical path length through the lens or an equivalently minimum electric phase resulting from Eq. (5).

Now, the index profile of each plane can be exactly calculated by using Eq. (1) through the above-discussed process, depending to the rising angle α and the aperture diameter of each plane, $2d$.

In this Letter, a lens whose aperture is elliptical is chosen to provide a fan-beam radiation pattern. We consider the diameters of the elliptical aperture as $2a = 20$ cm and $2b = 10$ cm.

Figure 3 shows the trajectory of rays starting from the point source for some rising angles from $-90°$ up to $90°$ for one of the planes. It can be seen clearly that the endpoint of beam rays distributed uniformly at the output aperture.

The inhomogeneous index profiles for the three planes are shown in Fig. 4(a). As can be seen, the index profile of each plane is equal to one on the output aperture and also near the point of excitation. The refractive index of the designed lens, n, changes gradually from 1.00 to 1.81, and the refractive index of the cross axis is similar for all planes.

Each plane of the lens is simulated separately in 2D space by using line source feeding in the FDTD scheme. Figure 4(b) shows a snapshot of the electric field in three planes at a frequency of 10 GHz. It is seen that inside the lens, the wavefront emitted by the source is converted smoothly into a plane wave in proximity of the free-space boundary.

We consider a stepped index structure for the designed lens, as shown in Fig. 5. The CST software is used to validate the performance of this proposed index profile. A WR90 (0.9 inch × 0.4 inch) waveguide antenna is used to excite the designed lens as the source antenna. It is placed beside the lens antenna, as seen in Fig. 5, to radiate

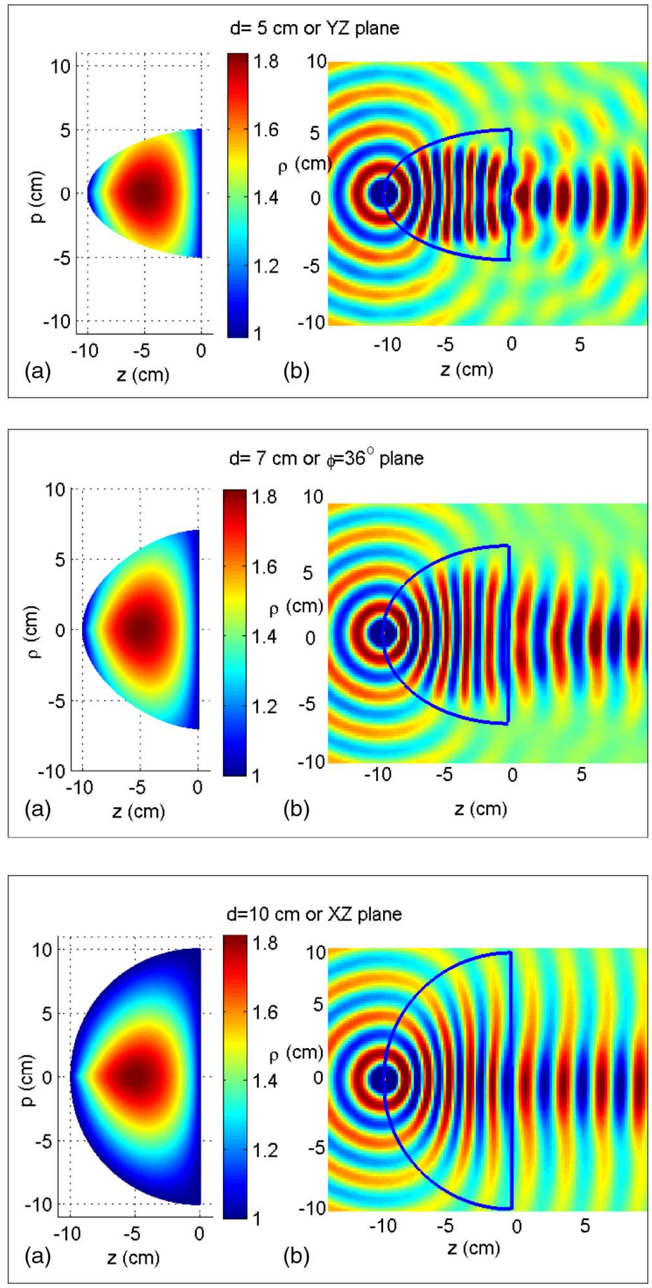

Fig. 4. (a) Refractive index profile and (b) electric field at 10 GHz.

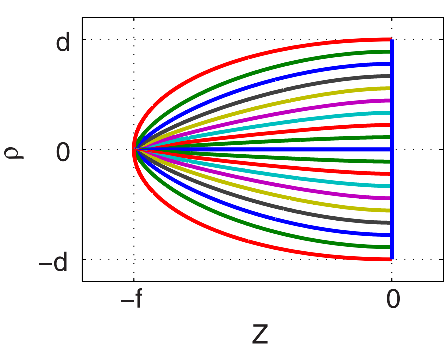

Fig. 3. Trajectory of beam rays that started from the point source.

a horizontally polarized wave. The reflection parameter, i.e., s11, of the structure is shown in Fig. 6. Because of the gradual change of the refractive index on the boundary of the lens, this structure has a very wide impedance-matching bandwidth.

Figure 7 shows the magnitude of the electric field distribution at a frequency of 10 GHz in the XZ and YZ planes. The radiation patterns of the feed source waveguide antenna and lens antenna at a frequency of 10 GHz are shown in Fig. 8. The directivity of the waveguide antenna at a frequency of 10 GHz is equal to 6.92 dBi with a half-power beam width of 63.3° in the H plane and 104.5° in the E plane. The radiation patterns

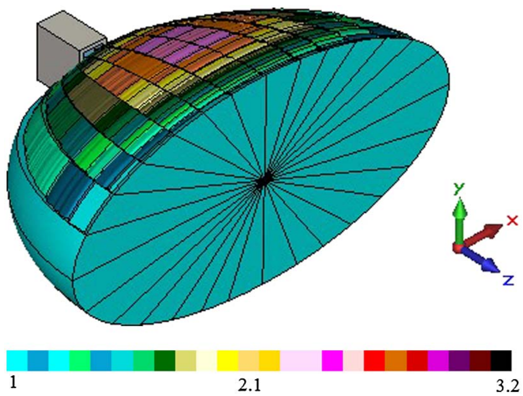

Fig. 5. Stepped index lens antenna exited by a waveguide.

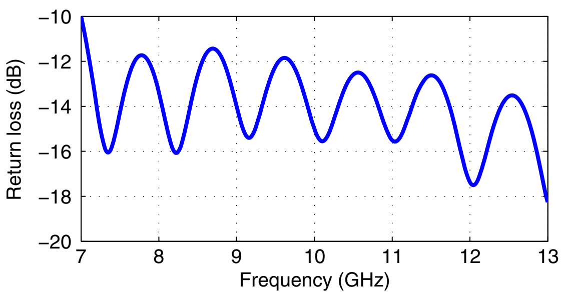

Fig. 6. Reflection loss of lens with WR90 antenna feeding.

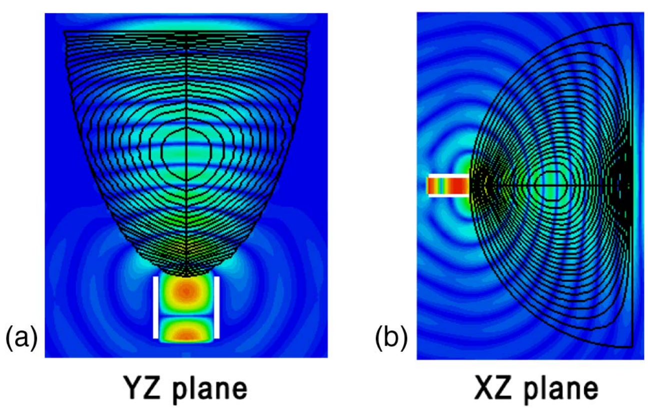

Fig. 7. Electric field at a frequency of 10 GHz.

of the waveguide antenna in E plane are wider in beam width than those in the H plane. The directivity of this lens antenna at a frequency of 10 GHz is equal to 20 dBi with a half-power beam width of 23° in narrow plane (vertical or H plane) and 12.5° in the wide plane (horizontal or E plane). The SLL is equal to 26.2 dB, and the back-lobe level is equal to 20.6 dB.

The simulated 3D radiation pattern of the lens is shown in Fig. 9 at a frequency of 10 GHz. Moreover, the radiation patterns at frequencies 9, 10, 11, and 12 GHz are shown in Fig. 10. The radiation efficiency of this structure is equal to 95.5%. It is seen that the beam width of the narrow plane is approximately twice the beam width of the wide

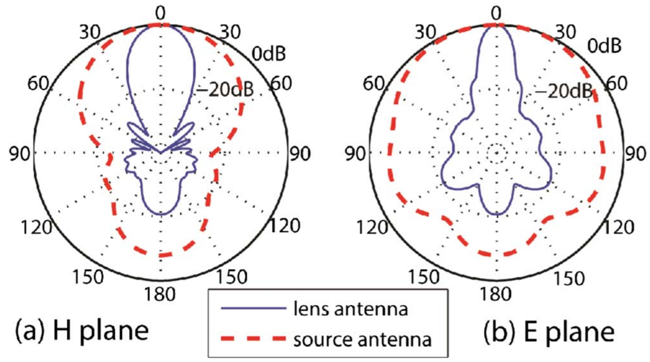

Fig. 8. Normalized radiation pattern of the lens antenna and source antenna at a frequency of 10 GHz. The directivity of the source antenna is 6.92 dBi and that of the lens antenna is 20 dBi.

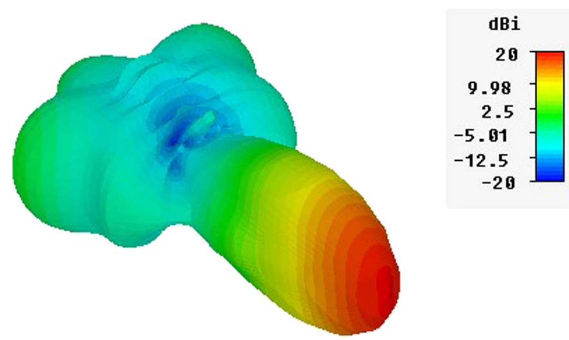

Fig. 9. 3D radiation pattern loss of lens with WR90 antenna feeding at a frequency of 10 GHz.

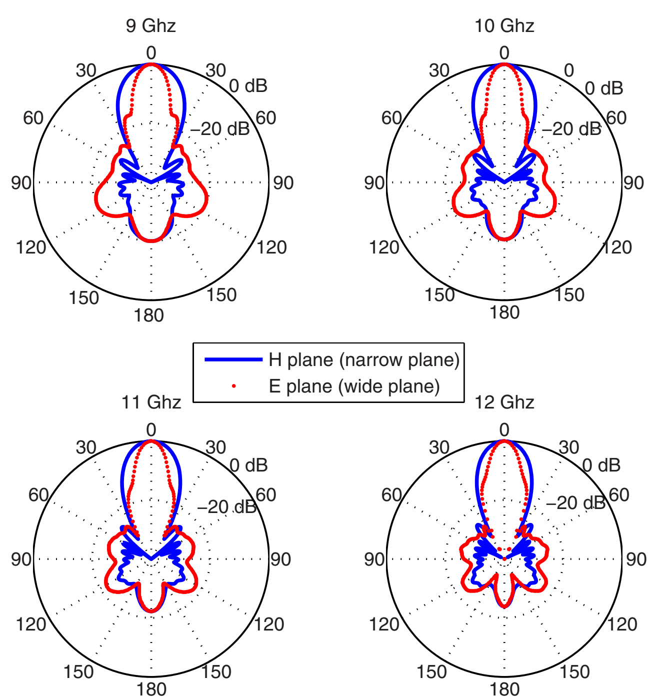

Fig. 10. Normalization radiation pattern of lens on E and H planes.

Table 1. 3D Lens Antenna's Pattern Information

Frequency (GHz)	Directivity (dBi)	SLL (dB)	Back Lobe Level (dB)	E plane half-power beam width EP-HPBW* (deg.)	H plane half-power beam width HP-HPBW* (deg.)	(HP-HPBW)/(EP-HPBW)
8	18.4	−16.5	−18.5	15	27.3	1.82
9	19.3	−20	−220	13.7	24.8	1.81
10	20	−26.2	−20.6	12.5	23	1.84
11	20.8	−22.2	−22.2	12	21.8	1.82
12	20.9	−23.9	−23.9	11.2	20.5	1.83

plane. So, this confirms that the vertical and horizontal planes of the radiation pattern can be determined independently to make the special fan-beam radiation pattern.

Table 1 shows the radiation pattern performances of the lens antenna excited by the WR90 waveguide at some frequencies. As seen from this table, and also in Figs. 6 and 9, this type of lens antenna can yield an arbitrary fan-beam radiation pattern and has an acceptable performance in a wide-frequency bandwidth and therefore can be used in both microwave- and millimeter-wave frequency bands.

This Letter presents an approach to designing a new kind of lens antenna that results in a suitable matching condition to the source antenna and surrounding environment and has a suitable fan-beam radiation pattern. It is assumed that the refractive index has a continuous and gradual change in the 3D model, so the index profile of the lens is calculated by solving the Eikonal equation on each plane crossed by the z-axis with some special conditions. It is proved that the trajectory of the beam rays in one plane determines the refractive index and is different from other planes related to the starting angle from the point source and end point of those rays. So, the vertical and horizontal planes of the radiation pattern can be determined separately to make the special fan-beam radiation pattern. It is main characteristic of this method, which was established from geometrical optics.

References

1. V. Kashin, A. Tumanskaya, and V. Shumilov, J. Commun. Technol. Electron. **57**, 972 (2012).
2. J. R. Costa, C. Fernandes, G. Godi, R. Sauleau, L. Le Coq, and H. Legay, IEEE Trans. Antennas Propag. **56**, 1251 (2008).
3. A. Bastawros, Opt. Commun. **58**, 235 (1986).
4. D. Ramaccia, F. Scattone, F. Bilotti, and A. Toscano, IEEE Trans. Antennas Propag. **61**, 2929 (2013).
5. H. Sakurai, T. Hashidate, M. Ohki, K. Motojima, and S. Kozaki, IEEE Trans. Electromagn. Compat. **40**, 94 (1998).
6. G. Godi, R. Sauleau, and D. Thouroude, IEEE Trans. Antennas Propag. **53**, 1278 (2005).
7. O. Lafond, M. Himdi, H. Merlet, and P. Lebars, IEEE Trans. Antennas Propag. **61**, 1672 (2013).
8. H. F. Ma and T. J. Cui, Nat. Commun. **1**, 124 (2010).
9. H. F. Ma and T. J. Cui, Nat. Commun. **1**, 21 (2010).
10. H. F. Ma, B. G. Cai, T. X. Zhang, Y. Yang, W. X. Jiang, and T. J. Cui, IEEE Trans. Antennas Propag. **61**, 5 (2013).
11. T. Driscoll, G. Lipworth, J. Hunt, N. Landy, N. Kundtz, D. N. Basov, and D. R. Smith, Opt. Express **20**, 13262 (2012).
12. C. Pfeiffer and A. Grbic, IEEE Trans. Antennas Propag. **58**, 3055 (2010).
13. M. Bosiljevac, M. Casaletti, F. Caminita, Z. Sipus, and S. Maci, IEEE Trans. Antennas Propag. **60**, 4065 (2012).
14. A. Mirkamali and J.-J. Laurin, in *2011 IEEE International Symposium on Antennas and Propagation (APSURSI)* (IEEE, 2011), p. 1773.
15. D. Smith, S. Schultz, P. Markoš, and C. Soukoulis, Physical Rev. B **65**, 195104 (2002).
16. A. Demetriadou and Y. Hao, Opt. Express **19**, 19925 (2011).
17. H. Mosallaei and Y. Rahmat-Samii, IEEE Trans. Antennas Propag. **49**, 60 (2001).
18. T. Komljenovic, R. Sauleau, Z. Sipus, and L. Le Coq, IEEE Trans. Antennas Propag. **58**, 1783 (2010).
19. C. Hua, X. Wu, N. Yang, and W. Wu, IEEE Trans. Microwave Theory Tech. **61**, 436 (2013).
20. L. Xue and V. Fusco, IET Microwaves Antennas Propag. **2**, 109 (2008).
21. L. Wu, X. Tian, H. Ma, M. Yin, and D. Li, Appl. Phys. Lett. **102**, 074103 (2013).
22. H. F. Ma, X. Chen, H. S. Xu, X. M. Yang, W. X. Jiang, and T. J. Cui, Appl. Phys. Lett. **95**, 094107 (2009).
23. R. K. Luneburg and M. Herzberger, *Mathematical Theory of Optics* (University of California Press, 1964).
24. B. Zhou, Y. Yang, H. Li, and T. J. Cui, J. Appl. Phys. **110**, 084908 (2011).
25. U. Leonhardt, Science **312**, 1777 (2006).
26. J. B. Pendry, D. Schurig, and D. R. Smith, Science **312**, 1780 (2006).
27. D. Schurig, New J. Phys. **10**, 115034 (2008).
28. K. Yao and X. Jiang, J. Opt. Soc. Am. B **28**, 1037 (2011).
29. R. E. Collin, *Antennas and Radiowave Propagation* (McGraw-Hill, 1985), chap. Appendix IV, p. 480.
30. A. Gutman, J. Appl. Phys. **25**, 855 (1954).